Environ Earth Sci (2017) 76:287
DOI 10.1007/s12665-017-6609-6

ORIGINAL ARTICLE

Terrestrial laser scanning monitoring and spatial analysis of ground disaster in Gaoyang coal mine in Shanxi, China: a technical note

Xugang Lian[1] · **Haifeng Hu**[1]

Received: 21 August 2016 / Accepted: 30 March 2017 / Published online: 6 April 2017

Abstract Monitoring ground disasters caused by underground mining has an important role in safe mining operations. In this study, terrestrial laser scanning (TLS) was performed to capture the point-cloud data of the slope landslide, ground steps and cracks, and tilt of a high-voltage tower during underground mining. The captured point-cloud data were processed by denoising, modeling, sectioning, and spatial analysis. TLS was also conducted to collect the point cloud of high-voltage towers in different mining periods, analyze the tilt degree of the towers, and estimate the stability of the tower body. The entire station was also used to collect the coordinates of single points around the study area. Two methods are compared, namely TLS monitoring and analysis, which is advantageous in describing the detailed local situation of a ground disaster, and total station monitoring, which focuses on absolute displacement monitoring of a single point. The monitoring process can combine both methods, including the absolute displacement and description of detailed status, thereby providing technical assistance to ensure mining safety. The monitoring solution has been applied in Gaoyang coal mine, which is located in Shanxi Province. Results show that the TLS method is more effective than the total station in capturing detailed spatial data on high-voltage towers and ground disasters such as landslides.

Keywords Terrestrial laser scanning · Spatial analysis · Mine ground disaster monitoring

✉ Xugang Lian
lianxugang@tyut.edu.cn

[1] School of Mining Engineering, Taiyuan University of Technology, Taiyuan 030024, Shanxi, China

Introduction

Underground coal mining operations can cause the movement and deformation of overlying strata and ground, thereby leading to different ground disasters such as ground cracks, collapse of pits, and landslides. The traditional measurement method involves setting up surface monitoring points along the advancing and dip direction of coal panel and obtaining the rules of ground movement and deformation caused by underground coal mining. The methods of sketching, taking photos, measuring geometric dimensions, and boundary surveying have been utilized to describe the status of ground disasters. Spatial data acquisition and shape description of ground disasters are currently a popular topic.

Experts and scholars have used interferometric synthetic aperture radar (InSAR) and global positioning system (GPS) technologies, as well as terrestrial laser scanning (TLS), and other methods or a combination of them, to explore land subsidence and landslide disasters. A geosensor network was used in mine ground disasters, which focused on the implementation of wireless sensor networks for real-time ground movement monitoring (Jin 2012; Salam et al. 2015). Synthetic aperture radar (SAR) is a popular technique to detect the deformation of focused objects. Polarimetric and interferometric ground-based synthetic aperture radar (Pol-GB-SAR, In-GB-SAR) system has been developed and applied to environmental monitoring and disaster prevention. The experimental results demonstrated that the system is highly efficient and can detect small changes of the scale of 2 cm at the range distance of 5 m (Hamasaki et al. 2005). Persistent scatter interferometry (PSI) technique was applied to retrieve the deformation rate, and the PSI results have been verified through leveling measurements, which indicate that this

PSI technique is an effective tool to monitor the reclamation-induced ground subsidence with high accuracy and adequate spatial details (Hu et al. 2013). Multiple SAR datasets were used to form independent interferometric stacks to unveil the spatial and temporal variations of land subsidence and ground fissures by using the time-series InSAR technique (Qu et al. 2014).

In GPS, a traditional positioning technique that was developed to monitor land disasters, the accuracy of vertical components had reached 2–4 mm (Xiao and He 2013). A GPS-enabled camera was used to conduct disaster damage assessment by capturing videos and pictures (Evan et al. 2014).

The SAR and GPS technologies can solve large-area ground deformation and perform high-accuracy positioning of single points, but these technologies are inadequate for the detailed 3D landform of ground disasters. TLS can rapidly collect the ground point clouds, thereby supplying the original data for any type of terrain feature space and ground disaster analysis. In addition, TLS point-cloud data were used to reconstruct a digital elevation model (Bing et al. 2015). The surface expression of three bedrock scarps, which results in the interaction between footwall incision, hanging wall sedimentation, channel incision, and landslides, as well as fault slips and linkages, was demonstrated by using combined datasets from ground-penetrating radar and TLS (Bubeckg et al. 2015). Furthermore, TLS can be used for landslides through multiple time-period scanning, and GPS data revealed detailed information on the occurrence of landslides (Yue et al. 2010; Syahmi et al. 2011; Zeybek and Sanlioglu 2015). Laser scanning data provide the height of ground objects, which can be used to develop models that can extract man-made features in a complex urban environment. By applying the height variation along the periphery of objects presented in the data, a method based on standard deviation was developed to distinguish between trees and buildings (Dash et al. 2004). An integrated survey using topographic, photogrammetric, and TLS techniques was conducted to obtain a 3D model of buildings, plans, and prospects, as well as the particulars of a collapsed area (Costantino and Angelini 2015), which can clearly capture the 3D information of the buildings. The TLS method can be used in post-disaster damage assessment; it is a rapid and detailed means of detecting the situation of damaged objects, as in tornado damage assessment (Kashani et al. 2015), and post-earthquake damage assessment (Chang and Wang 2012; Wilkinson et al. 2012; Pesci et al. 2013; Bonali et al. 2014).

Although InSAR can be used to monitor the subsidence in a wide area, the monitoring precision cannot reach the millimeter level. The GPS can precisely obtain the plane position for a single point, but the monitoring precision of vertical displacement remains insufficient. Both the InSAR and GPS technologies cannot describe the spatial characteristics of ground disasters in detail, and cannot conduct 3D modeling and spatial analysis for landslides, ground steps and cracks, and special constructions.

As a data collection method, TLS can quickly obtain the point-cloud data on ground disasters. The spatial data on ground disasters, such as displacement, subsidence, and slope change, can also be extracted rapidly. The 3D model can be established and spatial analysis can be conducted. This study mainly focuses on data collection of TLS and spatial characteristic analysis of point clouds for landslides, ground cracks, and construction damage due to underground mining, thereby providing a new way to monitor and assess ground disasters.

TLS monitoring landslide caused by underground mining

Mining plan and ground disasters in Gaoyang coal mine, Shanxi Province

Figure 1 shows the study area located in Gaoyang coal mine, Lvliang City, Shanxi Province in China. The ground above the extracted coal panel is mountainous terrain, and the relative height difference is approximately 130 m. The width of the coal panel is 200 m, the average extracted depth is 330 m, the thickness of the coal seam is 8.7 m, and the loess layer thickness ranges from 66 to 123 m.

During the extraction process, the ground disasters are formed, including collapse sinkholes, minor landslips, step crack groups, major landslides, major steps and cracks, ground upheaval, and minor ground cracks. The locations are shown in Fig. 2a–g, and the corresponding images are presented in Fig. 3.

Laser scanning and analysis of major landslide

The major landslide in Gaoyang coal mine was selected as a scanning and monitoring object (Fig. 2d). Scanning the landside was conducted under two conditions. First was on March 11, 2016, when the advancing distance of the working face was 518 m and the status of the slope beyond location D was 100 m, as shown in Fig. 4a. The second was on April 7, 2016, when the advancing distance was 568 m and the status of the slope beyond location D was 160 m, as shown in Fig. 4b. With regard to the accuracy of the scanning instrument, the measuring precision of the angle is $1''$, the measuring precision of distance is 0.6 mm + 1 ppm, and the scanning precision is 2 mm + 2 ppm in the range between 0 and 500 m.

Processed point-cloud data obtained from the aforementioned two scans through point-cloud denoising,

Fig. 1 Study area: Gaoyang coal mine in Shanxi Province, China

triangular network modeling, contour generation, profile processing, and formed visual surface of the 3D model of the landslide are shown in Fig. 5. Three profile analyses show that on April 7, as a result of extensive mining activities, massive soil on top of the slope slid and covered the slope surface that was formed on March 11.

The slope is the grade of a topographic feature or constructed element, namely, the ratio of vertical height to horizontal distance. According to the grade of the landslide, the different colors in the figure intuitively indicate the expressions of the terrain slope. As shown in Fig. 6a, the color on the top part of the slope is red, which illustrates that the slope is large and has a large potential collapse trend. Comparison of Fig. 6a and b shows that the slope of the largest part of the landslide on March 11, 2016, had reached 80°, and on April 7, 2016, the slope at 80° of the landslide was reduced due to the steep soil that slid down. Furthermore, the potential energy of the slope was reduced and the entire slope tended to be stable.

Total station monitoring on landslide

The detailed characteristics of the landslide were described by the point-cloud data from laser scanning and obtained the relative displacement of the landslide, but the absolute displacement can be obtained through total station monitoring of the points around the slope. The layout of monitoring points is shown in Fig. 4b. The top of the slope has two points: W14 and O16. The bottom of the slope has three points: W12, O13, and O14. The horizontal displacement of each point is shown in Fig. 7, the value of point O14 in dip direction is maximized at 7602 mm, whereas the distance between points O13 and O14 is only 30 m; the value of point O13 is 235 mm, which is very small compared with O14.

Point O14, which was affected by landslides, caused the horizontal movement on the foot of the slope. Point O16, located on top of the slope and at the horizontal displacement in the dip direction, was also disturbed very slightly at 1394 mm. In addition, point W11 was located at the

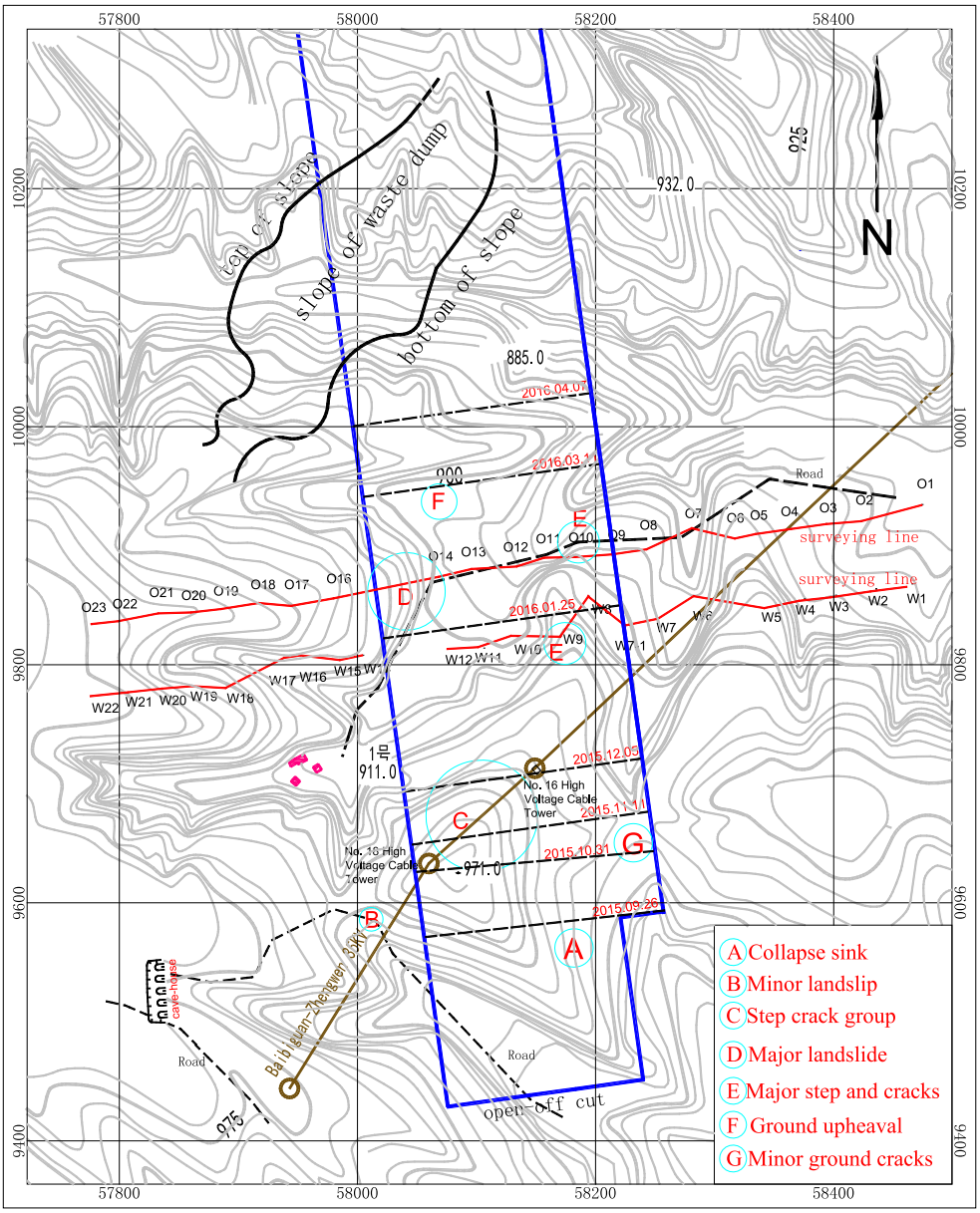

Fig. 2 Working face advancing schedule and layout of ground disaster and surveying lines

bottom of the slope and was affected by the slope sliding. The horizontal displacement in advancing direction was reached at 4666 mm, point W12 was far from the slope, and the horizontal movement was 1731 mm in the advancing direction.

Two observation lines are located in the dip direction of the working face (Fig. 8). Before January 25, 2016, the subsidence of the two lines was small, and the advancing position was only under line W. On March 11, 2016, with the working face advancing and passing line O at approximately 70 m, the surface subsidence occurred significantly. As the working face continued to advance, the change of subsidence on the ground was small. In line W, the subsidence between points W10 and W13 was larger at more than 4200 mm. The maximum subsidence point of 5686 mm was at W11, which was located at the center of the coal panel in the dip direction. The subsidence of point W17 was abnormal because of the gully between points W18 and W17, and point W17 was located at the slope, which was affected by the slope slipping. The horizontal distance between lines O and W was 50 m, and the subsidence of points between O10 and O14 was larger at more than 3000 mm. The maximum subsidence point O14, which was located in the center of the goaf, reached 5710 mm. In all observations of line O, the subsidence of point O11 is smaller because point O11 is located at the

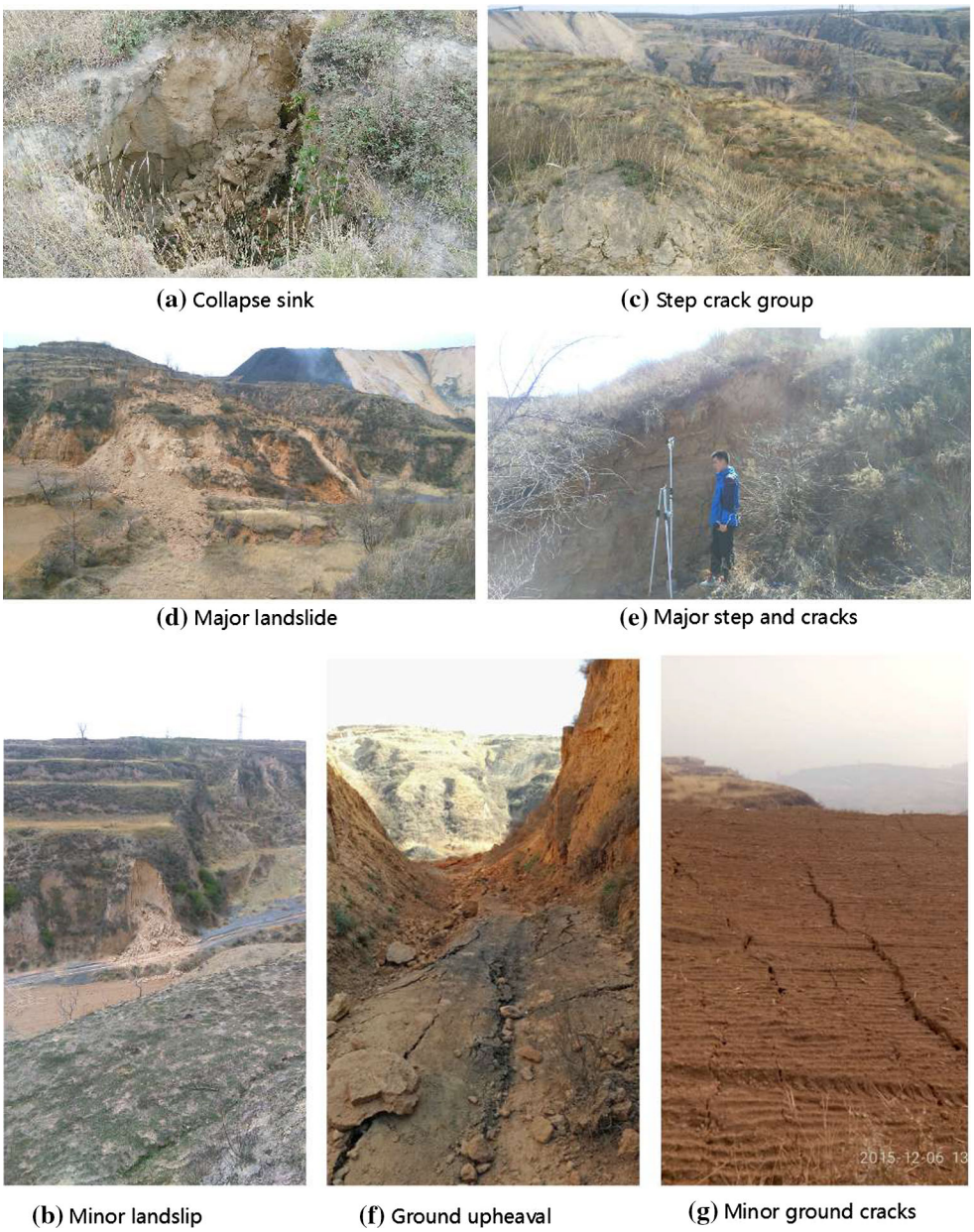

Fig. 3 Photographs of different ground disasters

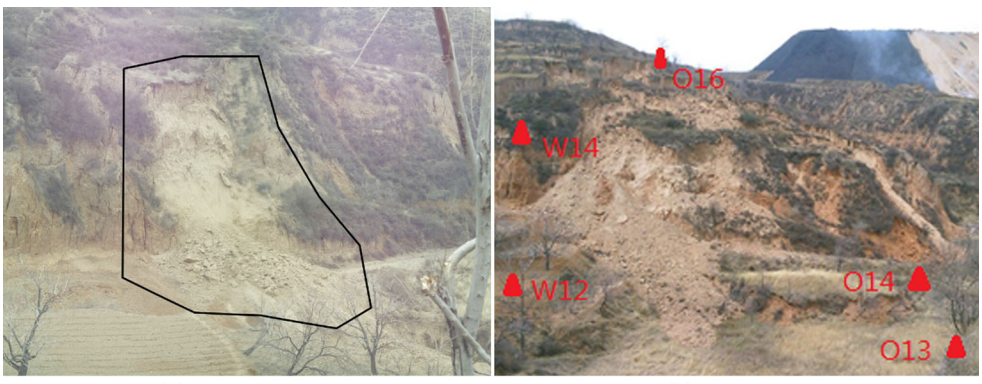

Fig. 4 Landslide at location D on different dates

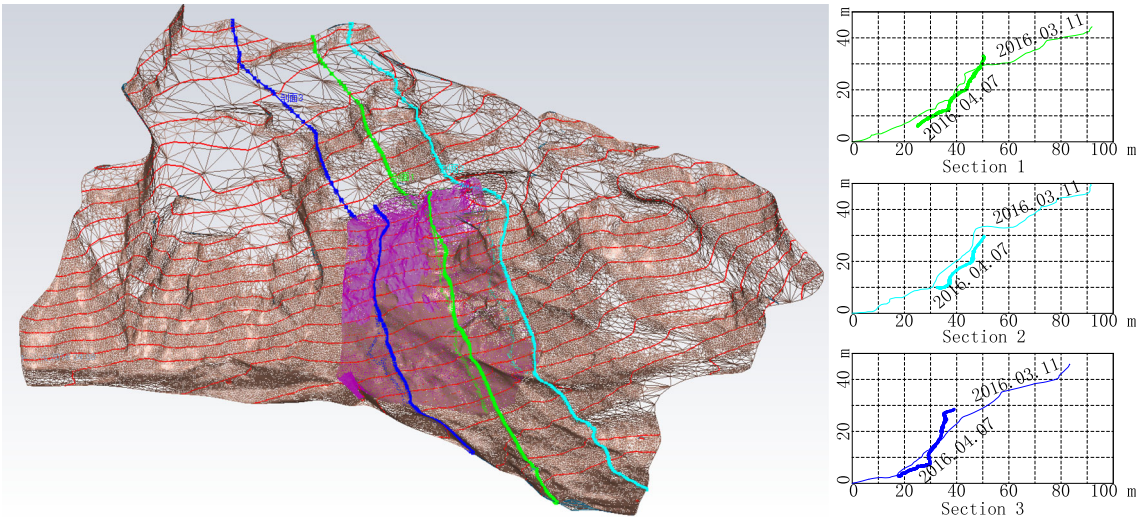

Fig. 5 Triangular irregular network model and section analysis for landslide

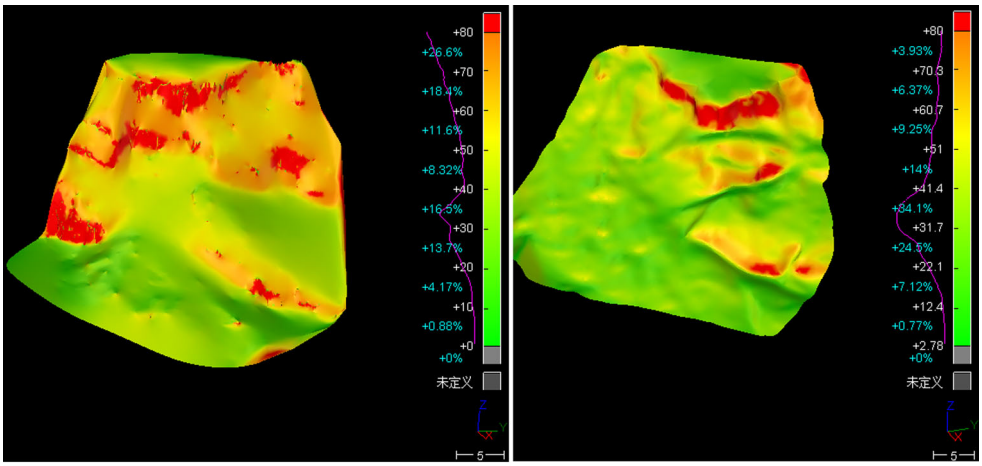

Fig. 6 Color maps of slope on different dates

(a) March 11, 2016 **(b)** April 7, 2016

bottom of the slope, and the horizontal movement is approximately 600 mm. Thus, a visible slip rupture at the field causes the point uplift at a certain degree.

Laser scanning on step crack caused by underground mine

As the working face advanced, the step cracks on the ground were also formed (Fig. 9). To monitor and determine the absolute movement and detailed characteristics of the step cracks, the total station and a laser scanner were utilized. The crack, as shown in Fig. 9a, is located near point W9 and on top of the slope, and the crack-step, as shown in Fig. 9b, is located near point O10 and at the bottom of the slope. According to Fig. 1, points W9 and O10 are on one line in advancing direction, and the main movement types are horizontal in advancing direction and subsidence (Fig. 10). The horizontal movement values of the two points along the advancing direction are similar because they are located on the same slope. The subsidence of point O10 is larger than that of point W9, and the difference is approximately 1500 mm.

To record the geometric shape of the step crack in detail, the site shown in Fig. 9b was scanned, and the point-cloud data of the step crack were obtained. Furthermore, the 3D model of the step crack was obtained through point-cloud denoising, modeling, and sectioning.

TLS is utilized to monitor the detailed characteristics of the step crack, which can accurately and fully collect the crack spatial information, and extract the sections in different locations to obtain the width of the crack and the height of the step. Three sections were extracted from Fig. 11a and b. On the basis of the section lines, the crack width is 2.04 m and the step height is 1.09 m in "Introduction" Section, the crack width is 1.70 m and the step

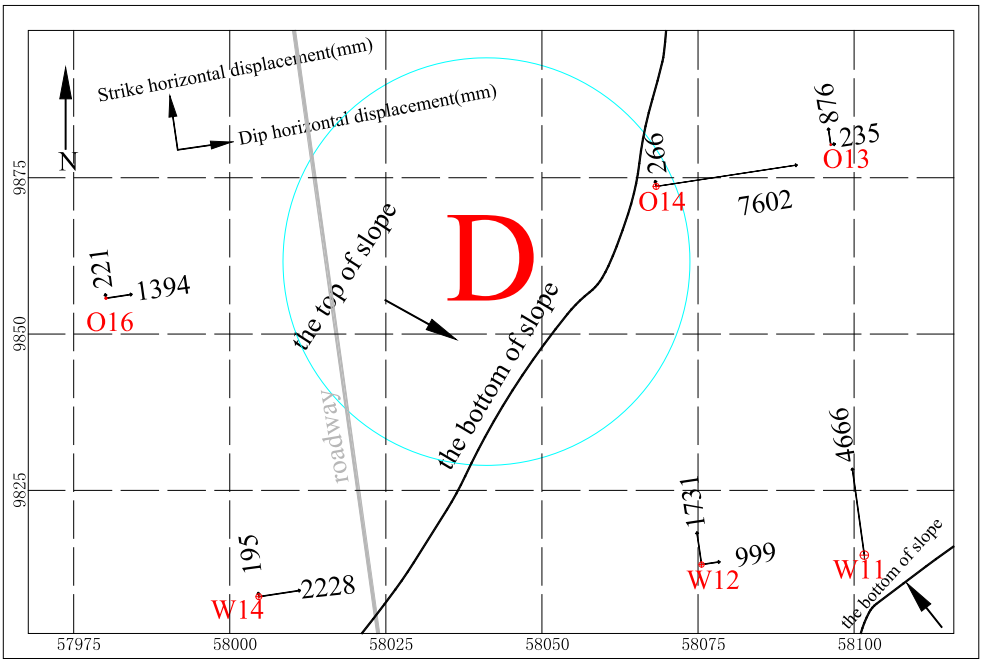

Fig. 7 Horizontal displacement of surveying points around landslide

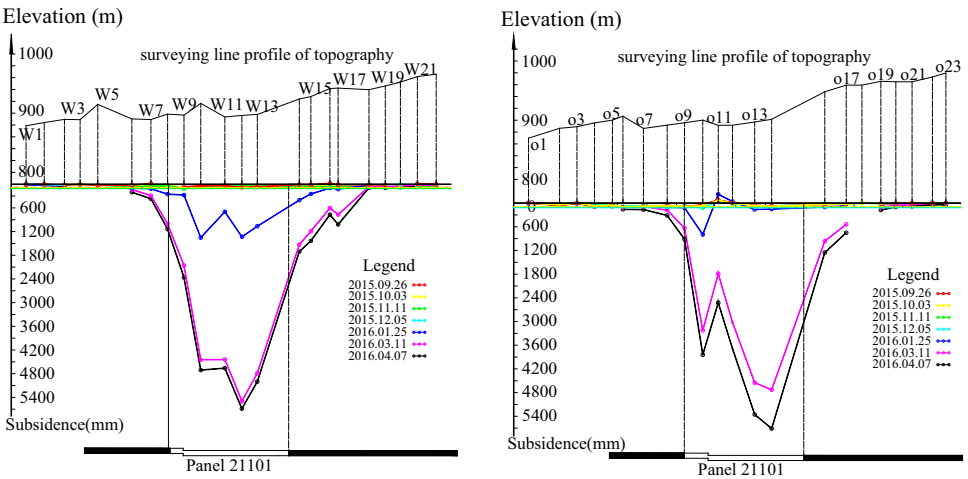

Fig. 8 Subsidence curves of W and O surveying lines during coal panel advancing

height is 2.12 m in "TLS monitoring landslide caused by underground mining" Section, and the crack width is 0.82 m and the step height is 2.11 m in "Laser scanning on step crack caused by underground mine" Section.

Laser scanning monitoring of high-voltage tower tilt caused by underground coal mining

Movement analysis of tower body

The No. 16 tower in Baibiguan–Zhengwen, which has a 35-kV high-voltage cable, is located above the underground coal panel. The movement and deformation of the tower during mining operations was monitored to prevent its collapse. The laser scanner was used to collect the point-cloud data on November 11, 2015, December 5, 2015, March 11, 2016, and April 8, 2016. The field picture and point cloud for each scan are shown in Fig. 12.

To determine the absolute movement of the tower, three surveying control points were set up outside the disturbed area induced by underground mining. When scanning the tower, the coordinates of based points were transferred from outside control points by traverse surveying. Two scanning-based points were set up around the tower: one at 90 m south and the other at 90 m northeast. Through traverse surveying, the accuracy of scanning-based points can

(a) Crack near point W9 **(b)** Step crack near point O10

Fig. 9 Surface step cracks caused by underground mining

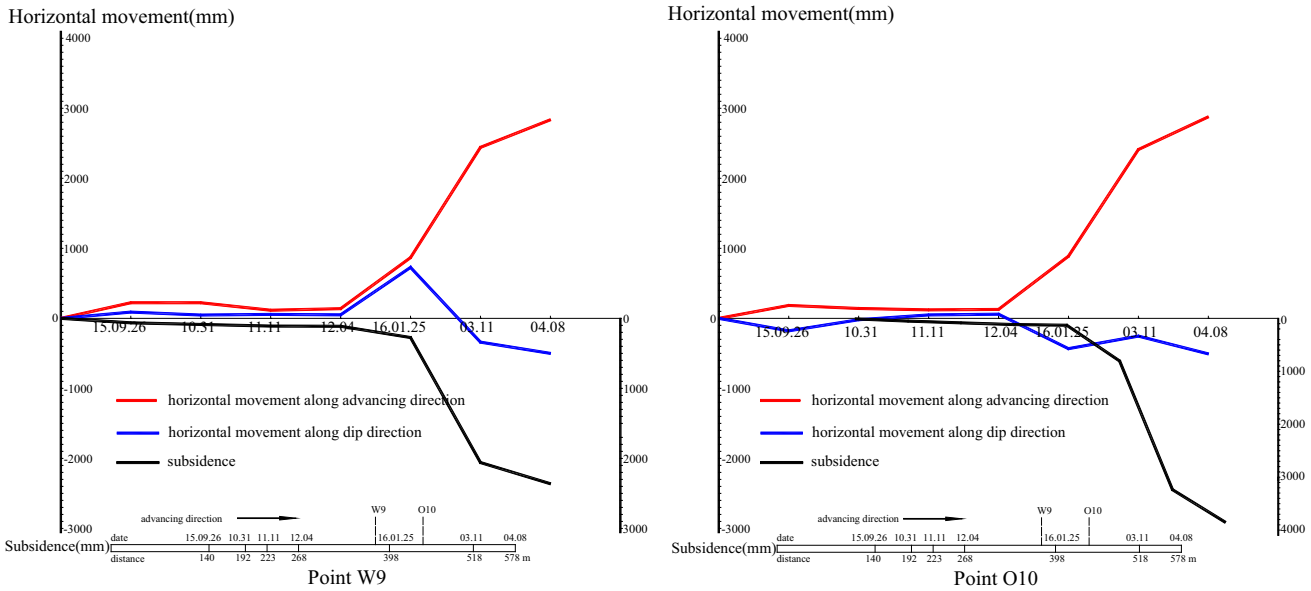

Fig. 10 Movement of points W9 and O10

reach the millimeter level. Both the vertical and horizontal resolution ratios are 1 cm.

According to the point-cloud data in Fig. 12b, on December 5, 2015, when the working face advanced to 268 m, it was located under the tower; the tower tilted and its body was distorted. After the tower was repaired, on March 11, 2016, when the working face advanced to 518 m, the working face passed the tower horizontal distance at 250 m, and the tower exhibited subsidence at 6.5 m along with a certain degree of horizontal movement, but the tower body was basically vertical. On April 8, 2016, when the working face advanced to 578 m and passed the tower at 310 m, the laser scanning results show a minimal difference from the previous comparison, which illustrates that the high-voltage tower has been stable. A comparison of the point cloud from the first to the fourth stage is presented in Fig. 12c; after the point-cloud denoising and feature-point matching, the subsidence is 6.74 m and the

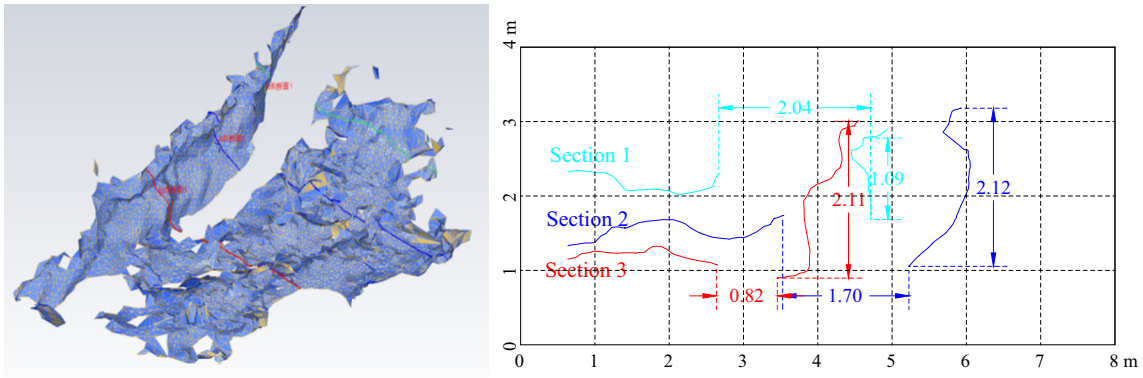

(a) 3D model **(b)** Sections

Fig. 11 3D model and sections of step crack

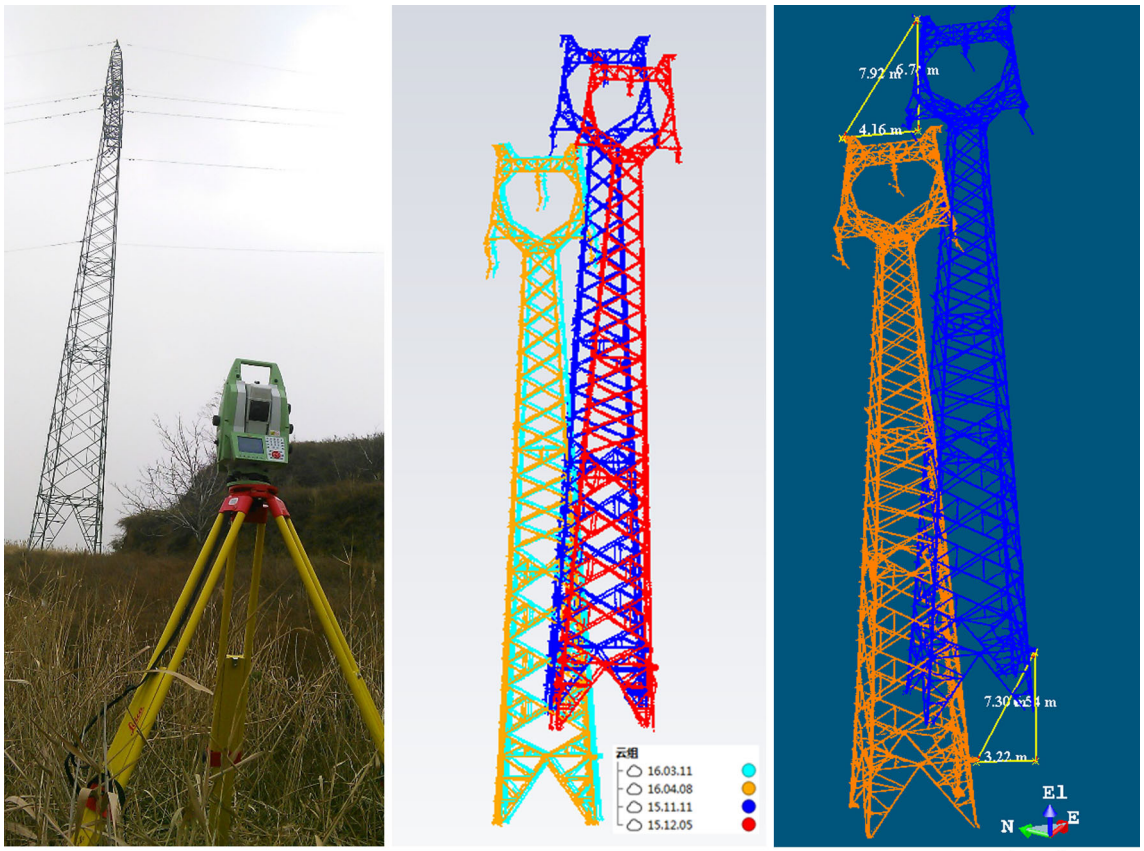

(a) Field photo **(b)** Point cloud at four time points **(c)** Point cloud from 1st to 4th stage

Fig. 12 No. 16 high-voltage tower

horizontal displacement is 4.16 m for the top of the tower, and the subsidence is 6.54 m and the horizontal displacement is 3.22 m for the bottom of the tower.

Tilt analysis of tower body

The center line from the top to the bottom of the tower body should be vertical, but the tower body tilted because of the underground mining. Through extraction of the center point coordinates of the top and bottom of the tower, the tilt can be calculated as follows:

$$\text{Tilt} = \frac{\sqrt{(x_t - x_b)^2 + (y_t - y_b)^2}}{H_{\text{tower}}},$$

where (x_t, y_t) are the horizontal coordinates of the center point of the top tower; (x_b, y_b) are the horizontal

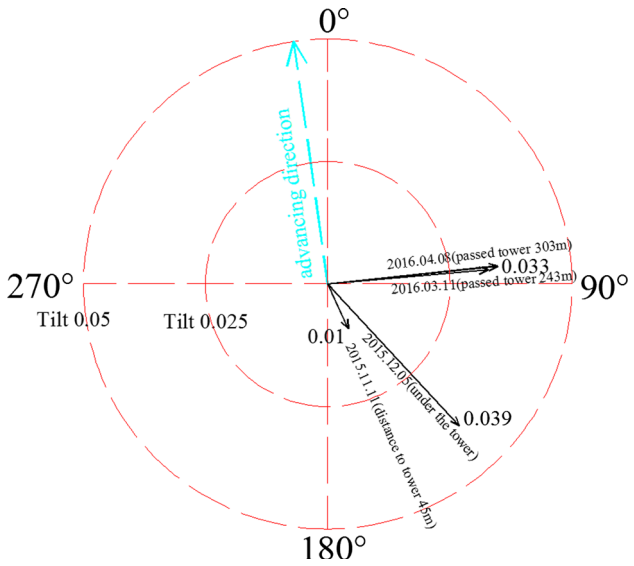

Fig. 13 Tilt change of tower body during mining

coordinates of the center point of the bottom tower; and H_{tower} is the height of the tower.

Based on a tilt calculation formula, the point cloud of four scanning times can obtain the following results: tilt on November 11, 2015 = 0.01, tilt on December 5, 2015 = 0.039, and tilt on March 11 and April 8, 2016 = 0.033. According to the "Operation Rules for Overhead Transmission Lines DL/T 741-2010," the electric power industry standard published by the National Energy Board of China, the tower height is less than 50 m and the allowed tilt is 1%. Therefore, Fig. 13 shows the changes in tower tilt during mining, which illustrates the tilt of the tower, and is larger than 1% after December 5, 2015. Thus, the tower has been protected by the pulling steel cable. In Fig. 13, the tilt azimuth can be found, which is useful in locating the position of the pulling steel cable.

Conclusions

The TLS method was used to monitor the ground disasters caused by underground mining, including landslide, step cracks, and tilting of high-voltage tower. By collecting the point-cloud data, 3D modeling, and spatial analysis, the following conclusions can be obtained:

(1) TLS can be used to collect the detailed spatial information of the landslide, and the traditional surveying method cannot be performed. Obtaining the same feature points from point-cloud data in two different periods in a landslide disaster is difficult; thus, obtaining the absolute movement of the landslide is also difficult. The total station is advantageous in monitoring the single point and obtaining high-accuracy absolute movement. Therefore, in the landslide monitoring project, combining TLS and total station is a good solution to obtain detailed spatial information and high-accuracy single point.

(2) Using TLS to scan the large-scale ground step cracks is convenient. On the basis of point-cloud data, TLS can extract the geometric shape in an arbitrary section. Furthermore, the crack width and height of the step can be measured easily.

(3) TLS can be used to monitor the tilt of the high-voltage tower. On the basis of the initial unaffected control points and through traverse surveying, the absolute movement of the tower can be obtained. The tilt of the tower can be calculated according to the tilt degree of the center line from the top to the bottom of the tower.

Acknowledgements Many thanks to the editor and reviewers, they help me improve the English of this paper. This study is supported by National Natural Science Foundation of China (Award Number: 51574132) and Gaoyang coal mine site in Shanxi Province. Thanks to all the surveyors in this project, they delivered 8 times surveying results.

References

Bing S, Zheng N, Li D et al (2015) Reconstructing DEM using TLS point cloud data and NURBS surface. Trans Nonferrous Met Soc China 25(9):3165–3172

Bonali E, Pesci A, Casula G et al (2014) Deformation of ancient buildings inferred by terrestrial laser scanning methodology: the Cantalovo church case study (Northern Italy). Archaeometry 56(4):703–716

Bubeck A, Wilkinson M, Roberts GP et al (2015) The tectonic geomorphology of bedrock scarps on active normal faults in the Italian Apennines mapped using combined ground penetrating radar and terrestrial laser scanning. Geomorphology 237:38–51

Chang KT, Wang EH (2012) Developing procedures for post-earthquake structural evaluation by laser scanning techniques. INSIGHT 54(10):562–567

Costantino D, Angelini MG (2015) Three-dimensional integrated survey for building investigations. J Forensic Sci 60(6):1625–1632

Dash J, Steinle E, Singh RP et al (2004) Automatic building extraction from laser scanning data: an input tool for disaster management. Adv Space Res 33(3):317–322

Depeng YUE, Jiping W, Jinxing Z et al (2010) Monitoring slope deformation using a 3-D laser image scanning system: a case study. Min Sci Technol 20(6):898–903

Hamasaki T, Ferro-Famil L, Pottier E et al (2005) Applications of polarimetric interferometric ground-based SAR (GB-SAR) system to environment monitoring and disaster prevention. Eur Radar Conf 29–32. doi:10.1109/EURAD.2005.1605556

Hu B, Wang H, Jiang L (2013) Monitoring of reclamation-induced ground subsidence in Macao (China) using PSInSAR technique. J Cent South Univ 20(4):1039–1046 **(English Edition)**

Jin Z (2012) Mine ground disaster precision monitoring geosensor networks and data processing. In: International symposium on mine surveying

Kashani AG, Crawford PS, Biswas SK et al (2015) Automated tornado damage assessment and wind speed estimation based on terrestrial laser scanning. J Comput Civ Eng 29(3):04014051(1–10)

Lue E, Wilson JP, Curtis A (2014) Conducting disaster damage assessments with spatial video, experts, and citizens. Appl Geogr 52(3):46–54

Pesci A, Teza G, Bonali E et al (2013) A laser scanning-based method for fast estimation of seismic-induced building deformations. ISPRS J Photogramm Remote Sens 79(4):185–198

Qu F, Zhang Q, Lu Z et al (2014) Land subsidence and ground fissures in Xi'an, China 2005–2012 revealed by multi-band InSAR time-series analysis. Remote Sens Environ 155:366–376

Salam RA, Islamy MRF, Munir MM et al (2015) Design and implementation of wireless sensor network on ground movement detection system. In: 2015 International conference on computer, control, informatics and its applications (IC3INA)

Syahmi MZ, Aziz WAW, Zulkarnaini MA et al (2011) The movement detection on the landslide surface by using terrestrial laser scanning. In: control and system graduate research colloquium (ICSGRC), 2011 IEEE, 27–28 June 2011. doi:10.1109/ICSGRC.2011.5991851

Wilkinson MW, McCaffrey KJW, Roberts GP et al (2012) Distribution and magnitude of post-seismic deformation of the 2009 L'Aquila earthquake (M6.3) surface rupture measured using repeat terrestrial laser scanning. Geophys J Int 189(2):911–922

Xiao R, He X (2013) Real-time landslide monitoring of Pubugou hydropower resettlement zone using continuous GPS. Nat Hazards 69(3):1647–1660

Zeybek M, Şanlıoğlu İ (2015) Accurate determination of the Taşkent (Konya, Turkey) landslide using a long-range terrestrial laser scanner. Bull Eng Geol Environ 74(1):61–76